Catalysis Letters 7 (1990) 1–14

THE QUANTUM CHEMICAL BASIS OF THE FISCHER-TROPSCH REACTION

R.A. VAN SANTEN *, A. DE KOSTER and T. KOERTS

Schuit Institute of Catalysis, Laboratory of Inorganic Chemistry and Catalysis,
Department of Chemical Engineering, Eindhoven University of Technology, Den Dolech 2,
5600 MB Eindhoven, The Netherlands

Fischer-Tropsch synthesis, transition metal surfaces, CO and CH_x reactivity, electronic features in F-T synthesis, bond strength, activation energy, chemisorption, CO dissociation, extended Hückel method, ASED method, quantum chemistry.

The electronic features determining the reactivity of CO and CH_x on transition metal surfaces are reviewed. Focus is on the relevant features that control the Fischer-Tropsch synthesis. The CO dissociation reaction path is controlled by the interaction with the CO bond strength weakening $2\pi^*$ orbitals. CH_3 fragment adsorption is controlled by σ type molecule fragment orbitals. This directs the CH_3 fragment to the atop adsorption site on those late transition metals that have strongly interacting d-valence electrons. Adsorbed C and O have a stronger bond strength than CH_3 because they have also unoccupied atomic p orbitals available to bonding. Because the bond strength of adsorbed C and O increases more rapidly with depletion of d-valence electron occupation than that of CO, the activation energy for CO dissociation decreases for the corresponding transition metals towards the left of the periodic system. The rate of methanation versus chain growth is controlled by the strength of the M–CH_3 bond versus the activation energy of carbon-carbon bond formation. The first appears to be more sensitive to variations in metal carbon bond strength than the latter.

1. Introduction

To heterogeneous catalytic synthesis gas conversion reactions the behaviour of chemisorbed CO is essential. On metal surfaces that have a high activation energy of CO dissociation, methanol will be produced. If dissociation is an easy reaction methane or higher hydrocarbons become produced [1a]. Whereas CO dissociation is the rate-limiting step in the Fischer-Tropsch reaction catalysed by Rh [1b], hydrogenation of chemisorbed C_nH_m species may be the rate limiting step on Co or Ni [2,3]. The thermodynamics of CO dissociation is determined by the difference in adsorption energy of chemisorbed CO and chemisorbed carbon and

---

* Paper presented in part at symposium on Fundamentals and Application of Fischer-Tropsch Synthesis AIChE Spring National Meeting, Orlando, March, 1990.

oxygen atoms. The activation energy of the dissociation reaction depends on details of the surface reaction path. In catalysis a different activation barrier for dissociation is measured dependent on conditions. If the surface coverage of CO is high, the apparent activation energy for CO dissociation is the difference in energy of the transition state complex of CO and chemisorbed CO. However if the surface coverage of CO is low, the activation energy has to be measured with respect to the gas phase. The order of the reaction in gas phase CO partial pressure is nearly zero in the first case, but close to one in the second case.

We will discuss the electronic basis of CO chemisorption for so far as relevant to an understanding of the factors that determine the activation energy of the dissociation reaction. Then the electronic basis of chemisorbed CH_x species and their reactivity will be analysed. For most of the results we will base ourselves on the use of the Extended Hückel method [4], or a modified version of the Extended Hückel method, the ASED method [4d] that introduces an empirical repulsive potential so that optimum configurations can be determined. Whereas the bond strength of molecular CO chemisorbed to different transition metals does not differ very much, the bond strengths of chemisorbed O or C atoms vary significantly [5]. This can be readily understood on the basis of the Bond-Order Conservation principle [6]. CO bonded with a carbon atom to the metal surface is bonded more weakly than an isolated C atom, because in the case of CO the metal-carbon bond order has to be shared with that of CO. Since the bond strength of the chemisorbed atoms tends to decrease when the transition metal d-valence electron band becomes filled the tendency to dissociate CO decreases for the transition metals with nearly filled d-valence electron bonds.

Quantum chemistry makes determination of the reaction path for CO dissociation possible. We will show that it provides the electronic basis to the ensemble effect [7].

Apart from a discussion of bonding of CH_x fragments we will also discuss the factors that determine recombination of CH_x fragments.

2. Quantum chemistry of CO and CH_x chemisorption

We will first discuss some of the essential features of bonding of CO to a transition metal surface and subsequently chemisorption of CH_x fragment species and C and O atoms.

Chemisorption of CO can be understood on the basis of the interaction of highest occupied 5σ and lowest unoccupied $2\pi^*$ CO orbitals with the metal surface orbitals. This is illustrated with the simplified scheme sketched in fig. 1. Fig. 1 is concerned with the interaction of CO with the d-atomic orbitals on a single metal-surface atom, thought to be decoupled from the other metal-atoms and completely filled with d-valence electrons. Cu would be an example.

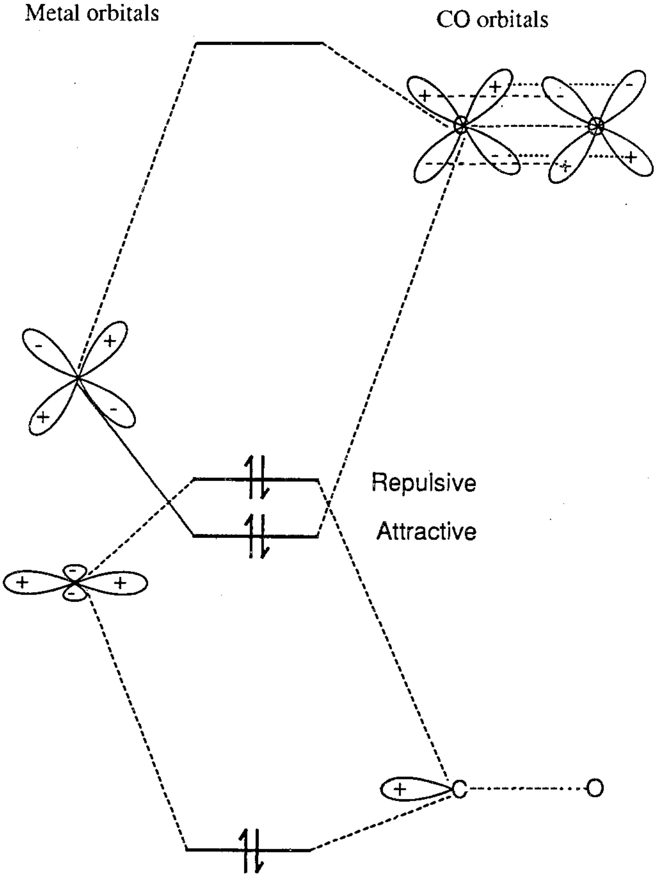

Fig. 1. Interaction of metal orbitals with orbitals of CO (schematic); above: Interaction of d_{xz} of metal atom with $2\pi^*$ of CO, below: Interaction of d_{z^2} of metal atom with σ of CO.

The highest occupied molecular of orbital of CO, the 5σ orbital, forms a bonding and anti-bonding molecular orbital pair with the filled Cu d_{z^2} orbital. Bonding as well as anti-bonding orbitals are doubly occupied. This results in a repulsive interaction proportional to $S^2_{d_{z^2}5_\sigma}$ [8–10], $S_{d_{z^2}5_\sigma}$ is the overlap of the metal d_{z^2} orbital and the CO 5σ orbital. The situation is different for interaction of the Cu d_{xz} or d_{yz} orbitals with the CO $2\pi^*$ orbitals. Again bonding and anti-bonding pairs of orbitals are formed. But now only the bonding orbital is doubly occupied and an attractive interaction results.

On the transition-metal surface the metal-surface atomic orbitals participate in delocalized metal orbitals. The d-valence electron band is only partially filled. There is also a significant interaction with the metal s- and p-valence electrons [4,8,9]. The detailed distribution of the electrons over the bonding and anti-bonding orbital fragments that are formed between adsorbate and metal surface determines the relative stability of adsorption complexes.

The bonding nature of the orbital fragments between chemisorbed molecule and surface metal atoms can be best analysed from the bond-order overlap-population densities [4,8–10] π_{ij}. i and j label the atomic or fragment molecular orbitals between which π_{ij} is calculated. π_{ij} is a function of the electron-energy. For low values of the energy π_{ij} has a positive sign. The corresponding orbital

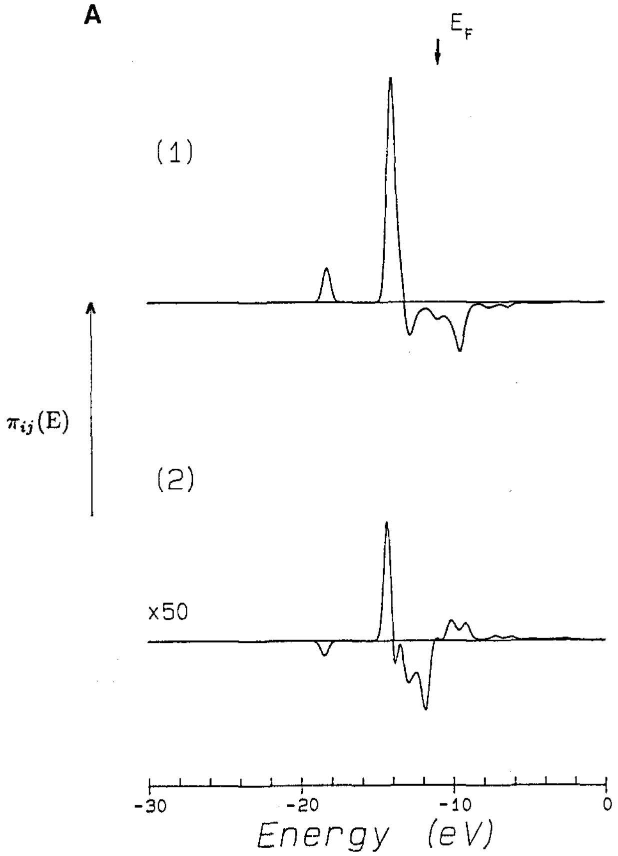

Fig. 2. Bond-order group-orbital overlap-population densities of CO with surface metal orbitals on Rh(111)

$$\alpha=\frac{1}{\sqrt{2+2S}}, \quad \beta=\frac{1}{\sqrt{2-2S}}$$

A. (1) CO 1 fold $d_{z^2}-5\sigma$
   (2) CO 2 fold $[\alpha(d_{z^2(1)}+d_{z^2(2)})]-5\sigma$
   (3) CO 2 fold $[\beta(d_{xz(1)}-d_{xz(2)})]-5\sigma$
   (4) CO 2 fold $[\alpha(d_{(x^2-y^2)(1)}+d_{(x^2-y^2)(2)})]-5\sigma$
B. (1) CO 1 fold $d_{xy}-2\pi^*$
   (2) CO 2 fold $[\alpha(d_{xz(1)}+d_{xz(2)})]-2\pi^*$
   (3) CO 2 fold $[\beta(d_{z^2(1)}+d_{z^2(2)})]-2\pi^*$
C. (1) CO 1 fold $s-5\sigma$
   (2) CO 2 fold $[\alpha(s(1)+s(2))]-5\sigma$
   (3) CO 2 fold $[\beta(s(1)-s(2))]-2\pi^*$.

fragment has a bonding contribution to the bond energy. If negative, π_{ij} has a bond weakening anti-bonding nature. Fig. 2 shows the bond-order overlap-population densities π_{ij} as computed for CO chemisorbed atop to a surface atom of a 28 atom cluster consisting of Rh atoms. The Extended-Hückel method has been used [4].

One observes that most orbital interactions are bonding, but that the Fermi level (the highest occupied orbital) is located in the anti-bonding area of $\pi_{d_{z^2},5\sigma}$. For Cu the Fermi level would have been such that bonding as well as anti-bonding $d_{z^2},5\sigma$ orbital fragments were occupied. Depletion of the anti-bonding orbital fragment area reduces the repulsive interaction [4,8–10]. Decreasing the anti-bonding fragment-orbital electron occupation converts the repulsive interaction in an attractive one.

This bonding model for chemisorbed CO, has some similarity to the well known Blyholder model [11], but contains also essential differences. The similarity is the loss of electron occupancy of CO 5σ electrons and the increase in electron occupation of CO $2\pi^*$ orbitals. The difference is the emphasis placed on

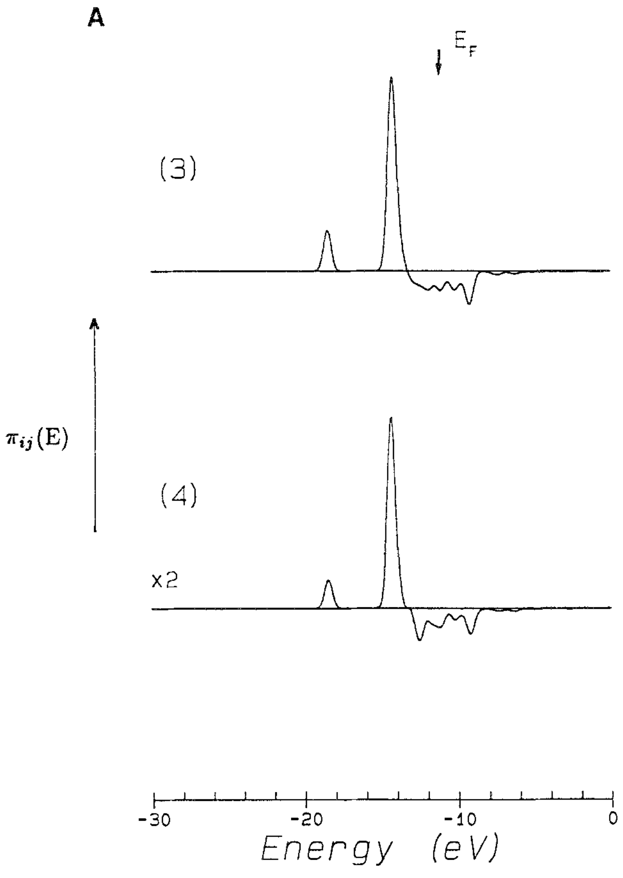

Fig. 2A. (continued).

considering bonding as well as anti-bonding-orbital fragment pairs and their electron-occupation. Secondly it is very important to include the overlap S explicidly in the consideration, so that Pauli repulsion is properly included. We have argued elsewhere [10,12] that the repulsive interaction between doubly occupied atomic-orbitals is to lowest order in S proportional to the number of nearest-neighbour atomic orbital atom pairs:

$$E_{\mathrm{rep}} \approx 4fNS^2 \tag{1}$$

N being the number of surface atoms that coordinate to the occupied adsorbate atomic orbital. f is the partial occupation of the surface atomic orbitals concerned. Strictly expression (1) is valid only for s type orbitals. However also for doubly occupied degenerate orbitals relation (1) may be expected to hold. For doubly occupied degenerate atomic orbitals the electron distribution is spheric.

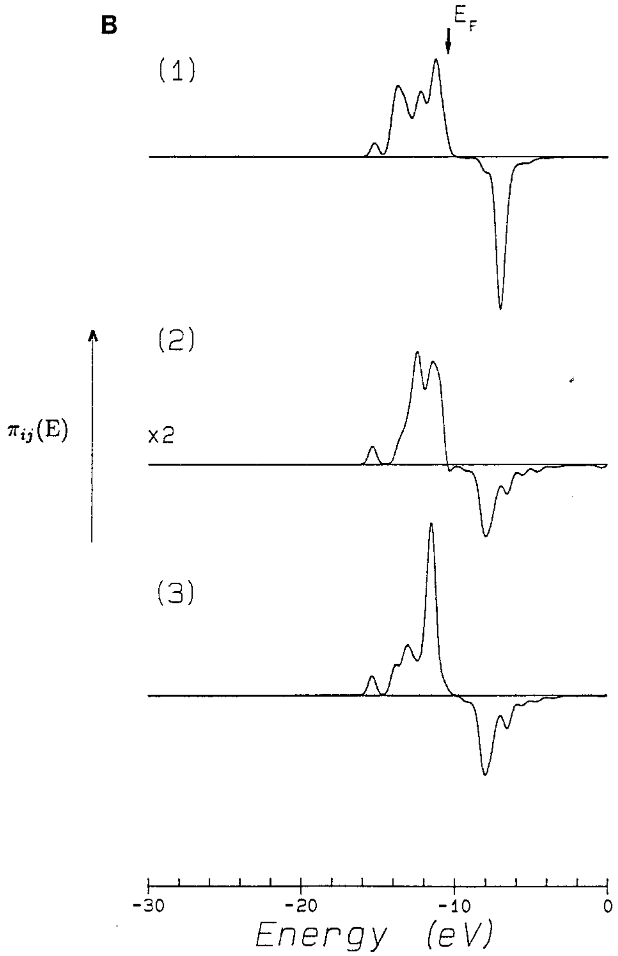

Fig. 2B.

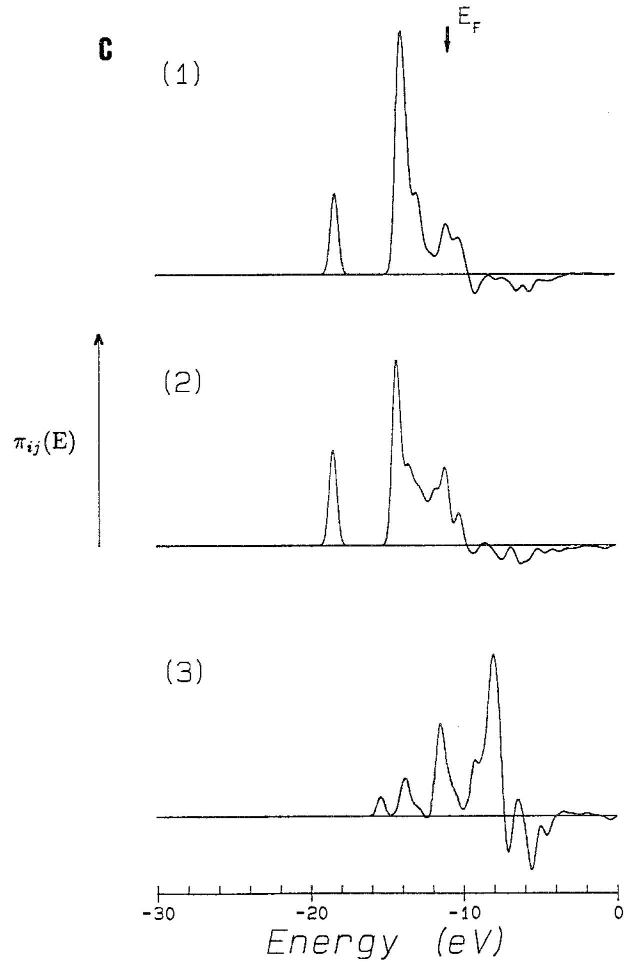

Fig. 2C.

On the Cu surface CO prefers a top coordination, because then the repulsive interactions with the completely filled d-valence electrond band are minimized [12,13].

On Ni the d-valence electron band is not completely filled and as a result the repulsive interaction decreases. On Ni surfaces atop coordination is not anymore the most favoured coordination site [14]. The interaction with the $2\pi^*$ orbital is bonding for the whole range of possible d-valence electron occupancies. Therefore it favours coordination to higher coordination sites. It is the slight dominance of this interaction on Ni that shifts CO to the bridge position. The two effects together cause the bond strength of CO to increase from Cu to Ni. On Co further depletion of d-valence electron bond shifts CO again to the atop position [15]. For the CO 5σ orbital the interaction with d-valence electrons has (now) become attractive. It appears that a strong σ type interaction with highly

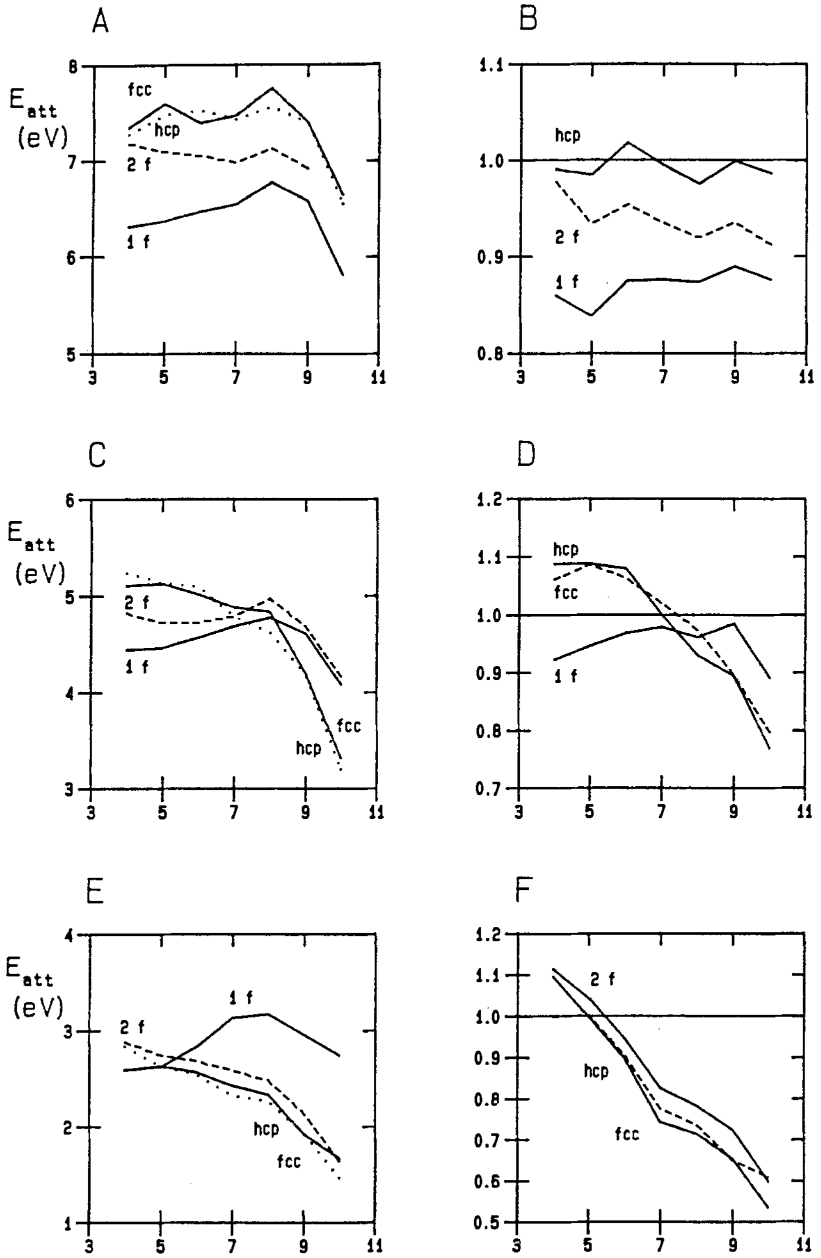

Fig. 3. Adsorption energy (E-attraction) and ratio of adsorption energy on an x-fold site to that of the preferred y-fold site [$E(x\text{f}/y\text{f})$] of CH_x ($x=1, 2, 3$) on Rh(111).

A. E attraction of CH adsorbed 1-fold, 2-fold, 3-fold fcc and 3-fold hcp on Rh(111).

B. The ratio of the adsorption energy of CH adsorbed on 1-fold and 2-fold sites to that of CH on 3-fold sites.

C. E-attraction of CH_2 adsorbed at 1-fold, 2-fold, 3-fold fcc and 3-fold hcp on Rh(111).

D. The ratio of the adsorption energy of CH_2 adsorbed on 1-fold and 3-fold sites to that of CH_2 adsorbed on 2-fold sites.

E. E-attraction of CH_3 adsorbed at 1-fold, 2-fold, 3-fold fcc and 3-fold hcp on Rh(111).

F. The ratio of the adsorption energy of CH_3 adsorbed on 2-fold and 3-fold sites to that of CH_3 adsorbed on 1-fold sites.

Table 1
Adsorption of CH_3 on Ni(111): influence d orbital size

ζ_2	site	E_{tot} (eV)	$E_{att}^{(1)}$ (eV)	$h_x^{(2)}$ (Å)
1.9	1-fold	−4.41	−4.88	2.0
	2-fold	−4.01	−4.67	1.7
	3-fold fcc [3]	−3.96	−4.44	1.7
	3-fold hcp [4]	−3.95	−4.43	1.7
2.0	1-fold	−4.47	−5.27	1.9
	2-fold	−4.24	−4.90	1.7
	3-fold fcc [3]	−4.22	−4.94	1.6
	3-fold hcp [4]	−4.23	−4.95	1.6
2.1	1-fold	−4.49	−5.29	1.9
	2-fold	−4.41	−5.06	1.7
	3-fold fcc [3]	−4.43	−5.15	1.6
	3-fold hcp [4]	−4.47	−5.19	1.6
2.2	1-fold	−4.49	−5.29	1.9
	2-fold	−4.52	−5.18	1.7
	3-fold fcc [3]	−4.58	−5.30	1.6
	3-fold hcp [4]	−4.64	−5.36	1.6

[1] Bond energy contribution excluding the two-body repulsion term
[2] Height of adsorbing species (X = C, H or CH_x) above the surface
[3] No Ni present in second layer
[4] Ni present in second layer

occupied d-valence orbitals always results in a favouring of the atop position [4,10,12]. Then the smallest electron occupancy of anti-bonding fragment orbitals occurs. Fig. 3 shows for chemisorbed CH_3 as a function of valence-electron occupation the ratio's of the atop, two-fold and three-fold coordinated total Extended-Hückel interaction energies. Rh orbital parameters are used. It is the interaction with the n-CH_3 lone pair orbital directed towards the metal that causes the shift to the atop position with increased d-valence electron occupation. Because the unoccupied π-type anti-bonding orbitals of the CH_3 bonds have a high energy, the back-donating interaction is very small. This changes of CH_2, CH and C. These hydrocarbons are more strongly bonded to Rh, mainly because of the availability of empty p-type adsorbate orbitals. At the end of the transition-metal series as long as the interaction with the d-valence electrons dominates, the hydrocarbon fragments choose a configuration that optimizes hybridization [4a,16]. CH_2 tends to favour two fold, CH three fold and C higher coordinations sites.

Only when the interaction with the d-valence electrons decreases and that with the bonding s, p valence electron band dominates CH_3 will also favour high coordination sites (table 1). For Ni(111) this is the experimentally favoured situation [17,18].

3. Quantum chemistry of CO dissociation

The difference in adsorption energy of atomic C and O and the chemisorption energy of CO defines the dissociation energy of chemisorbed CO. The activation energy is determined by the dissociation reaction path. The favoured dissociation paths on the Rh(111), Rh(110) and Rh(100) surface are sketched in fig. 4. The path of minimum energy is controlled by two factors:

1. The interaction between the C and O atoms generated upon dissociation has to be minimum.
2. Activation of the anti-bonding CO $2\pi^*$ orbitals.

Repulsive covalent interaction between adsorbed atoms occurs if they share bonds with the same surface atoms. Joyner e.a. [19] have shown that the electronic basis is the reduction of local density of states at the Fermi level on metal atoms involved in strong covalent bonds. That reaction path is favoured that minimize the number of surface-atoms shared between ad-atoms after dissociation. In order to dissociate the CO molecule the CO bond length has to stretch. The weaker the CO bond strength of adsorbed CO, the lower the barrier to dissociation. The bond strength of CO can be weakened by population of the anti-bonding CO $2\pi^*$ orbitals. This interaction will be optimum when the dissociating molecule moves side-on over a surface atom. The $2\pi^*$ orbital can then interact with anti-symmetric atomic d_{xz} and d_{yz} orbitals.

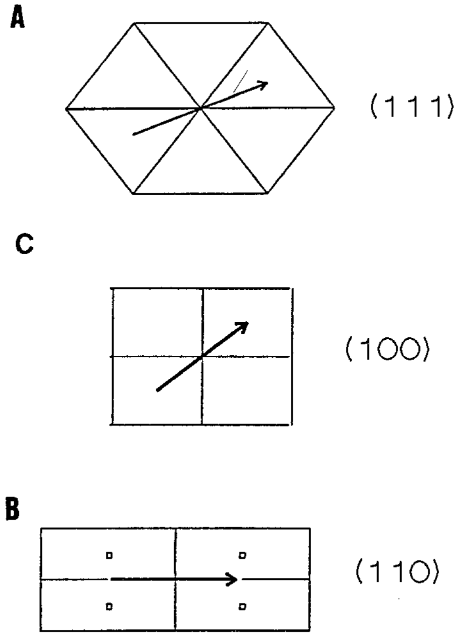

Fig. 4. Most favourable dissociation reaction path for CO on Rh(111) (A), Rh(100) (B) and Rh(110) (C).

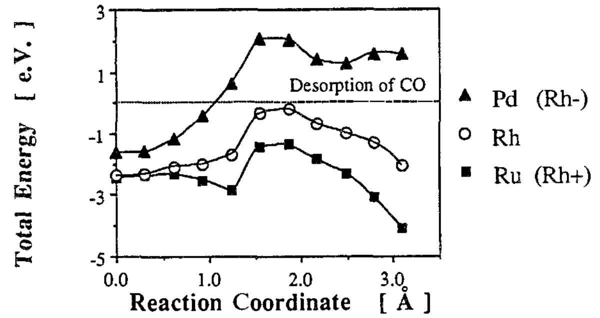

Fig. 5. Changes in CO dissociation activation energy as a function of valence electron occupation, on a fcc (111) surface of 40 metal atoms. Ru and Pd are created from Rh by respectively substraction or adding 1 electron from the valence electrons.

The general principles formulated for the CO dissociation path have probably a more general validity. The activation energy for recombination and dissociation is very often controlled by population or depopulation of anti-symmetric anti-bonding, repulsive orbital fragments. Destabilization of such an orbital requires interaction with anti-symmetric surface-group orbitals [20]. Surface d-orbitals centered at surface atoms provide such orbitals. Computed dissociation energies for the minimum activation energy path on the (111) surface as a function of metal valence electron occupation are shown in fig. 5. Again all parameters are chosen as for Rh, except for the metal valence electron occupation. The results presented in fig. 5 show clearly the small change in CO adsorption bond strength compared to that of adsorbed C and O. Noteworthy is the predicted increase in activation energy of CO dissociation with increased metal-atom electron occupation. One finds on Ru that CO in tilt position has a local minimum.

4. Carbon-carbon bond formation

The consequences for catalysis depend on the hydrogen partial pressure in equilibrium with the metal surface. In Ultra High Vacuum hydrocarbon fragments will be dehydrogenated and the question to be answered concerns the fate of the adsorbed atom species. Clearly if the metal-carbon interaction increases, carbon-carbon bond formation will become less exothermic. Besides it appears that the activation energy for recombination is only a weak function of the d-valence electron bond occupation. This is the result shown in fig. 6. Experimentally it is well known that carbides are formed by strongly interacting metals as Fe or W, but graphitic carbon may form on these metals (to the right of the periodic system) that more weakly interact with surface metal atoms. It has been

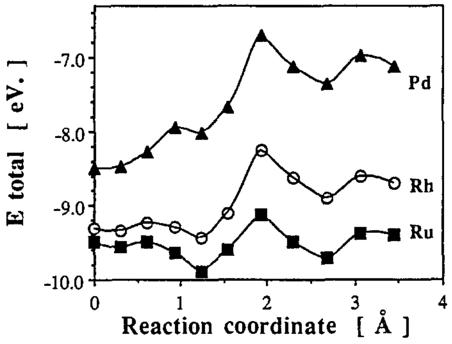

Fig. 6. Recombination of C and CH_2 fragments on Ru, Rh and Pd. (Reaction coordinate zero means CH_2 on top of the C atom.)

found that the active surface-phase under Fischer-Tropsch conditions is a Fe/C related phase [21].

The surface condition during the Fischer-Tropsch synthesis is largely determined by the hydrogen-partial pressure. Whether chain propagation, termination or methane formation occurs depends on the relative rates of hydrogenation versus carbon-carbon formation.

To form methane a CH_3 fragment has to be hydrogenated. Clearly this is thermodynamically mostly favoured on the metal with lowest metal-methyl bond strength, which is the case for transition-metal elements to the right of the periodic system.

As has been shown by Zheng, Apelag and Hoffmann [9], the activation energy for CH_x recombination is largely controlled by the repulsive interaction of the CH bonds. Such interactions decrease if recombination of CH_x species occurs with $x < 3$. Table 2 summarizes activation energies of recombination reactions

Table 2
Recombination of CH_x fragments on $Rh_{40}(111)$ surface

Atom	Moving species	E_{act} [eV]
C	CH_3	1.98
C	CH_2	0.98
C	CH	1.75
C	C	1.63
C	H	0.99
C	CO	1.35

$$\left.\begin{array}{l} CH+CH \\ CH+CH_2 \\ CH+CH_3 \\ CH_2+CH_2 \\ CH_2+CH_3 \\ CH_3+CH_3 \end{array}\right\}\text{Repulsive under tested condition.}$$

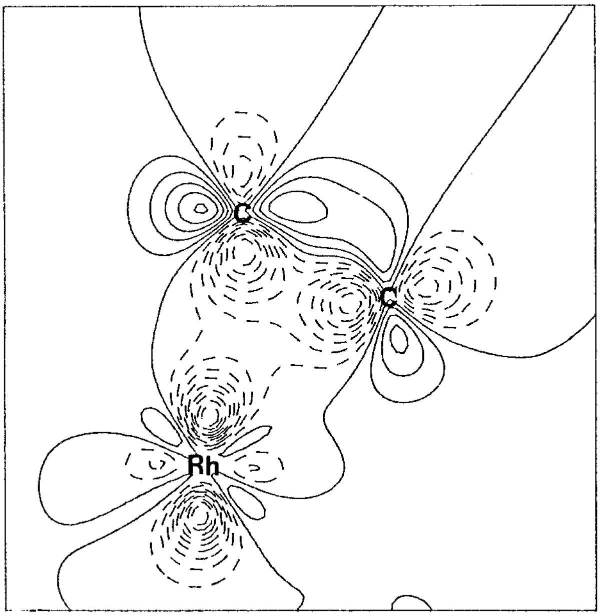

Fig. 7. Changes in electron density of C and CH_2 in the transition state during coupling on a Rh(111) surface. Calculated is the change in electron density by subtracting the electron density of the lose fragments (Rh_{11} cluster, CH_2 and C) from those of the Ru_{11}–C–CH_2 cluster. The dotted line connects points with the same electron density loss, the drawn line connect points with the same increase of electron density.

computed according to the ASED method [23] on the Rh(111) clusters. Reasonable values are found for low values of x.

Chain growth will be favoured over methanation on metals that have a significant surface coverage of reactive carbon [22] with a long residence time for adsorbed CH_x intermediates. This partially explains why metals with a relatively high dissociation energy of CO will produce a low surface coverage of reactive carbon. Therefore they tend to produce methane (Pd, Pt, Ir). An increase of the metal-carbon-strength will decrease the rate of hydrogenation of CH_3. An important difference between hydrogenation and hydrocarbon-fragment recombination is that in methanation new hydrogen-carbon bonds replace the broken metal-carbon band. In the chain growth reaction C–C bond formation requires only the rupture of metal-π type bonds. In fig. 7 the transition state shows large changes in electron density in the C–C bonding regime whereas a strong bond between metal and carbon atoms is maintained. Therefore the activation energy for chain growth will be less sensitive to changes in valence-electron-occupation than the surface bond strengths of partially hydrogenated hydrocarbon fragments. The relative increase in chain growth rate comparing Ni with Co or Pd with Rh and Ru is consistent with this analysis.

Also the recent observations of increased chain growth on Rh promoted with vanadium [24] seems to be in line with this. One observes an increased metal-carbon bond strength on Rh promoted with vanadium. Similarily on the more open Co surface, carbon atoms will be more strongly bonded than on the more dense surfaces. The open surfaces have been shown to have an increased propagation rate [22].

Clearly on reactive metals carbide formation will compete with propagation which may be the reason for the preference of d^9, d^8, transition metals for Fischer-Tropsch catalysis. The lower transition metals may form too stable carbides.

References

[1a] M. Araki and V. Ponec, J. Catal. 44 (1976) 439;
P. Biloen and W.M.H. Sachtler, Adv. in Catal. 30 (1981) 165.
[1b] Y. Mori, T. Mori, A. Miyamoto, N. Takahashi, T. Hattori and Y. Murakami, J. Phys. Chem. 93 (1989) 2039.
[2] R.C. Baetzold, J. Phys. Chem. 88 (1984) 5583.
[3] A.T. Bell, Catal. Rev. -Sci. Eng. 23 (1981) 23.
[4a] A. de Koster, thesis, Eindhoven University of Technology, The Netherlands, 1989.
[4b] A. de Koster and R.A. van Santen, J. Vac. Sci. Technol. A6 (1988) 1128.
[4c] A. de Koster, A.P.J. Jansen, J.J.C. Geerlings and R.A. van Santen, Faraday Discuss., Chem. Soc. 87 (1989) 263.
[4d] A.B. Anderson, J. Chem. Phys. 62 (1975) 1187.
[5] J.B. Benziger, App. Surf. Sci. 6 (1980) 105.
[6] E.M. Shustorovich, Surf. Sci. Rep. 6 (1986) 1;
E.M. Shustorovich, J. Am. Chem. Soc. 106 (1984) 6479.
[7] R.A. van Santen and W.M.H. Sachtler, Adv. Catal. 26 (1977) 69.
[8] S.-S. Sung and R. Hoffmann, J. Am. Chem. Soc. 107 (1985) 578.
[9] Ch. Zheng, Y. Apeloig and R. Hoffmann, J. Am. Chem. Soc. 110 (1988) 749.
[10] R.A. van Santen and E.J. Baerends, in: *Theoretical Models of Chemical Bonding*, ed. Z.B. Maksic, part 4 (Springer-Verlag) to appear.
[11] G. Blyholder, J. Phys. Chem. 68 (1964) 2772.
[12] R.A. van Santen, J. Mol. Struct. 173 (1988) 157.
[13] P. Hollins and J. Pritchard, Progr. Surf. Sci. 19 (1985) 275.
[14] J.C. Bertolini and B. Tardy, Surf. Sci. 102 (1981) 131.
[15] C. Backx and C.P.M. de Groot, unpublished results.
[16] C. Minot, M.A. van Hove and G.A. Somorjai, Surf. Sci. 127 (1982) 441.
[17] J. Schule, P. Siegbahn and U. Wahlgren, J. Chem. Phys. 89 (1988) 6982.
[18a] M.B. Lee, Q.Y. Yang, S.L. Tang and S.T. Ceyer, J. Chem. Phys. 85 (1986) 1693.
[18b] S.T. Ceyer, J.D. Beckerle, M.B. Lee, S.L. Tang, Q.Y. Yang and M.A. Hines, J. Vac. Sci. Technol. A4 (1987) 501.
[18c] M.B. Lee, Q.Y. Yang and S.T. Ceyer, J. Chem. Phys. 87 (1987) 2724.
[19] R.W. Joyner, J.B. Pendry, D.K. Saldin and S.R. Tennison, Surf. Sci. 138 (1984) 84.
[20] R.A. van Santen, Progress in Surf. Sci. 25 (1987) 253.
[21] J.W. Niemantsverdriet, A.M. van der Kraan, W.L. van Dijk and H.S. van der Baan, J. Phys. Chem. 84 (1980) 3363.
[22] J.J.C. Geerlings, M.C. Zonnevylle and C.P.M. de Groot, Catal. Lett. 5 (1990) 309.
[23] A.B. Anderson, R.W. Grimes and S.Y. Hong, J. Phys. Chem. 91 (1987) 4245.
[24] T. Koerts and R.A. van Santen, Catal. Lett. 6 (1990) 49.